Supporting Information

"Thermosensitive gate opening and selective gas adsorption in porous coordination nanocage"

Dan Zhao,[a] Daqiang Yuan,[a] Rajamani Krishna,[b] Jasper M. van Baten[b] and

Hong-Cai Zhou[*a]

[a] Department of Chemistry, Texas A&M University, College Station, Texas 77843,

USA

[b] Van 't Hoff Institute for Molecular Sciences, University of Amsterdam, Science

Park 904, 1098 XH Amsterdam, The Netherlands.

E-mail: zhou@mail.chem.tamu.edu

Experimental Details

Materials and methods. Commercially available reagents were used as received without further purification. Nuclear magnetic resonance (NMR) data were collected on a Mercury 300 MHz NMR spectrometer. Fourier transform infrared spectroscopy (FTIR) data were collected on a SHIMADZU IRAffinity-1 FTIR Spectrophotometer. Thermogravimetry analyses (TGA) were performed under N_2 on a SHIMADZU TGA-50 Thermogravimetric Analyzer, with a heating rate of 5 °C min^{-1}. Elemental analyses (C, H, and N) were obtained from Canadian Microanalytical Service, Ltd. Powder X-ray diffraction (PXRD) patterns were obtained on a BRUKER D8-Focus Bragg-Brentano X-ray Powder Diffractometer equipped with a Cu sealed tube (λ = 1.54178) at a scan rate of 0.2 s deg[-1], solid-state detector, and a routine power of 1400 W (40 kV, 35 mA).

Synthesis of diethyl 5-((triisopropylsilyl)ethynyl)isophthalate, 1. Diethyl 5-iodoisophthalate[1] (6.67 g, 19.16 mmol), Pd(PPh$_3$)$_4$ (555 mg, 0.48 mmol) and CuI (37 mg, 0.19 mmol) were mixed in a 500 mL three neck Schlenk flask. The flask was pumped under vacuum and refilled with N_2 for three times, and then 200 mL of freshly distilled and degassed triethylamine was added. The mixture was cooled to 0 °C in an ice water bath and ethynyltriisopropylsilane (5.24 g, 28.73 mmol) dissolved in 50 mL of THF was added via syringe dropwise. The mixture was stirred at room temperature for 1 hour, and then heated to reflux under nitrogen atmosphere overnight. After removal of organic solvent, the residue was dissolved in chloroform (150 mL) and washed with water (100 mL). The aqueous layer was back-extracted with chloroform (3 × 50 mL), and the combined organic layers were dried over MgSO$_4$ and filtered. The solvent was removed and the crude product was purified by column chromatography on silica gel with dichloromethane to give compound **1** as red oil (7.27 g, yield: 94 %). δ_H(300 MHz; CDCl$_3$; Me$_4$Si) 8.59

(1 H, t, *J* 3), 8.26 (2 H, d, *J* 3), 4.41 (4 H, q, *J* 6), 1.41 (6 H, t, *J* 6), 1.14 (18 H, m) and 1.08 (3 H, m);

δ_C(300 MHz; CDCl$_3$; Me$_4$Si) 165.17, 136.75, 131.06, 130.00, 124.36, 104.73, 93.06, 61.55, 18.61, 14.29

and 11.21; *m/z* (ESI) 121.071 (92 %), 263.113 (91 %), 293.131 (100 %) and 403.259 ([M+H$^+$], 43 %).

Synthesis of 5-((triisopropylsilyl)ethynyl)isophthalic acid, TEI. Compound 1 (7.649 g, 19 mmol)

was suspended in 150 mL of THF/methanol (1/1) mixed solvent, to which 100 mL of 1 M NaOH

aqueous solution was added. The mixture was stirred at room temperature for 1 hour. Organic solvent

was removed under vacuum, and diluted hydrochloric acid was added to the remaining aqueous solution

until it became acidic (pH = 2). The precipitate was collected by filtration, washed with water and dried

under vacuum at 80 °C to give TEI as white solid (5.261 g, yield: 84 %). v_{max}(neat)/cm^{-1} 2941, 2864,

2152, 1693, 1442, 1249, 952, 918, 881, 746 and 667; δ_H(300 MHz; DMSO-d_6; Me$_4$Si) 8.43 (1 H, d, *J* 3),

8.10 (2 H, t, *J* 3), 1.11 (18 H, m) and 1.10 (3 H, m); δ_C(300 MHz; DMSO-d_6; Me$_4$Si) 165.70, 135.66,

132.04, 129.93, 123.13, 104.92, 92.13, 18.39 and 10.59; *m/z* (ESI) 345.127 (M$^-$, 100 %) and 691.276

(37 %).

Synthesis of CuTEI. TEI (100 mg, 0.289 mmol) was dissolved in 200 mL of benzene/methanol (19/1)

mixed solvent, to which 2,6-lutidine (62 mg, 0.579 mmol) dissolved in 5 mL of methanol was added.

The solution was sonicated for 10 min to insure complete deprotonation. Cu(NO$_3$)$_2$·2.5H$_2$O (67 mg,

0.288 mmol) dissolved in 5 mL of methanol was added into the previous solution. The solution turned

into homogeneous deep blue. After precipitating and washing with methanol three times and drying

under vacuum overnight, the final product was isolated as deep blue powder, which is readily soluble in

several organic solvents, such as ether, benzene, chloroform, etc. Recrystallization from

chloroform/DMF afforded single crystal suitable for X-ray crystallography study. The product has a

formula of [CuTEI(CH$_3$OH)(H$_2$O)]$_{24}$, which is derived from crystallographic data, elemental analysis

(% calc/found: C 52.44/52.47, H 6.60/6.46), and TGA. v_{max}(neat)/cm^{-1} 2943, 2864, 2154, 1635, 1585,

1421, 1375, 881, 810, 771, 734 and 671.

X-ray crystallography. Single crystal X-ray structure determination of CuTEI was performed at 173(2) K on the Advanced Photon Source on beamline 15ID-B in Argonne National Laboratory. Raw data for the structure were processed using APEX-II and absorption corrections were applied using *SADABS*. Structures were solved by direct method and refined by full-matrix least-squares on F^2 using *SHELXTL*. Non-hydrogen atoms were refined with anisotropic displacement parameters during the final cycles. Organic hydrogen atoms were placed in calculated positions with isotropic displacement parameters set to $1.2 \times U_{eq}$ of the attached atom. The solvent molecules are highly disordered, and attempts to locate and refine the solvent peaks were unsuccessful. Contributions to scattering due to these solvent molecules were removed using the *SQUEEZE* routine of *PLATON*; structures were then refined again using the data generated. Due to the small crystal size, the diffraction remained weak even under synchrotron radiation, and it is not possible to obtain a significantly better crystallographic model using methods currently available. Although the data in hand are poor, we still believe they support our interpretation.

Crystal data for CuTEI: $C_{76}H_{104}Cu_4O_{20}Si_4$, $M = 1704.11$, trigonal, space group $R\text{-}3m$ $a = b = 51.642(5)$, $c = 33.245(4)$ Å, $V = 76783(14)$ Å^3, $Z = 18$, $D_c = 0.663$ g/cm^3, $F_{000} = 16056$, synchrotron radiation, $\lambda = 0.42318$ Å, $T = 173(2)$K, $2\theta_{max} = 24.6º$, 381539 reflections collected, 9447 unique ($R_{int} = 0.3749$). Final *GooF* = 3.422, *R1* = 0.4492, *wR2* = 0.7748. CCDC-779616.

Low-pressure gas sorption measurements. The low-pressure gas sorption isotherm measurements were performed on a Micromeritics ASAP 2020 surface area and pore size analyzer. Before measurements, the sample was degassed at 120 °C overnight to remove the coordinated ligands. UHP grade N_2, He, H_2, Ar, O_2, CH_4 and CO_2 were used for all measurements. Oil-free vacuum pumps and oil-free pressure regulators were used for all measurements to prevent contamination of the samples during the degassing process and isotherm measurement. The temperatures at 77 K, 87 K, 113 K, 142 K, 179 K, 195 K, and 273 K were maintained with a liquid nitrogen bath, liquid argon bath,

iso-pentane-liquid nitrogen bath, pentane-liquid nitrogen bath, hexane-liquid nitrogen bath, acetone-dry ice bath, and ice water bath, respectively.[2]

High-pressure gas adsorption and kinetics measurements. High pressure excess adsorption of H_2, CH_4 and CO_2 and H_2 sorption kinetics were measured using an automated controlled Sieverts' apparatus (PCT-Pro 2000 from Setaram) at 77 K (liquid nitrogen bath), 87 K (liquid argon bath) or 298 K (room temperature). About 1.7 g of activated sample was loaded into sample holder under an argon atmosphere. Before measurements, sample was degassed at 120 °C overnight. The free volume was determined by the expansion of low-pressure He (<5 bar) at room temperature. The temperature gradient between gas reservoir and sample holder was corrected by applying to the raw data a correction factor, which was obtained by replacing the sample with polished stainless-steel rod and measuring the adsorption isotherm at the same temperature over the requisite pressure regime. The sorption kinetics data were obtained via monitoring the pressure change in the sample holder once being connected to the gas reservoir. 80 bar of H_2 was used in the reservoir for adsorption kinetics study, and 70 bar of H_2 was used in the sample holder for desorption kinetics study.

Force fields, simulation methodology, and structural information. The CuTEI structure was considered to be rigid in the simulations. For the atoms in the host, the generic UFF[3] and DREIDING[4] force fields were used. The Lennard-Jones parameters for the framework atoms are summarized in Table S1. Figure S1 provides different perspectives of the pore landscapes. The areas that are accessible to the guest molecules are indicated in red. The adsorption isotherms for CH_4 and Ar were computed using Monte Carlo (MC) simulations in the grand canonical (GC) ensemble. CH_4 molecules are described with a united atom model, in which each molecule is treated as a single interaction centre.[5] The parameters for CH_4 are taken from Dubbeldam *et al.*[6] The force field for Ar corresponds to that given by Skoulidas and Sholl.[7] Additionally, Molecular Dynamics simulations were also carried out to determine the self-diffusivity of CH_4 within CuTEI for a variety of loadings. The Lorentz-Berthelot

mixing rules were applied for calculating σ and ε/k_B for guest-host interactions. The Lennard-Jones

potentials are shifted and cut at 12 Å. The number of unit cells in the simulation box was chosen such

that the minimum length in each of the coordinate directions was larger than 24 Å, 2 unit cells in each

direction. Periodic boundary conditions were employed. Further GCMC simulation details are available

in earlier publications.[6, 8] The GCMC simulations were performed using the BIGMAC code developed

by T.J.H. Vlugt as basis.

CO_2/CH_4 selectivity prediction *via* IAST. The experimental isotherm data for pure CO_2 and CH_4

obtained using PCT-Pro 2000 for the high-pressure range (measured at 298 K) were fitted using a

dual-Langmuir-Freundlich model:

$$q_i = q_{i,A,sat} \frac{b_{i,A} p_i^{v_{i,A}}}{1 + b_{i,A} p_i^{v_{i,A}}} + q_{i,B,sat} \frac{b_{i,B} p_i^{v_{i,B}}}{1 + b_{i,B} p_i^{v_{i,B}}}$$

(Eq. S1)

The adsorption selectivities, S_{ads}, for binary mixtures of $CO_2(1)$/$CH_4(2)$, defined by

$$S_{ads} = \frac{q_1/q_2}{p_1/p_2}$$

(Eq. S2)

were calculated using the Ideal Adsorption Solution Theory (IAST) of Myers and Prausnitz.[9] The

calculations for binary mixtures with equal partial pressures in the bulk gas phase, i.e. $p_1 = p_2$.

Where

b_i dual-Langmuir-Freundlich constant for species i, Pa^{-v_i}

p_i bulk gas phase pressure of species i, Pa

p_t total bulk gas phase pressure of mixture, Pa

q_i molar loading of species i, mol kg^{-1}

$q_{i,sat}$ saturation capacity of species i, mol kg^{-1}

S_{ads} adsorption selectivity, dimensionless

i exponent in the dual-Langmuir-Freundlich isotherm fits, dimensionless

A, B   referring to adsorption sites A, and B

sat   referring to saturation conditions

Reference

1. I. Aujard, J. P. Baltaze, J. B. Baudin, E. Cogné, F. Ferrage, L. Jullien, E. Perez, V. Prévost, L. M. Qian and O. Ruel, *J. Am. Chem. Soc.*, 2001, **123**, 8177-8188.
2. R. E. Rondeau, *J. Chem. Eng. Data*, 1966, **11**, 124.
3. A. K. Rappe, C. J. Casewit, K. S. Colwell, W. A. Goddard and W. M. Skiff, *J. Am. Chem. Soc.*, 1992, **114**, 10024-10035.
4. S. L. Mayo, B. D. Olafson and W. A. Goddard, *J. Phys. Chem.*, 1990, **94**, 8897-8909.
5. J. P. Ryckaert and A. Bellemans, *Faraday Discuss.*, 1978, 95-106.
6. D. Dubbeldam, S. Calero, T. J. H. Vlugt, R. Krishna, T. L. M. Maesen and B. Smit, *J. Phys. Chem. B*, 2004, **108**, 12301-12313.
7. A. I. Skoulidas and D. S. Sholl, *J. Phys. Chem. B*, 2002, **106**, 5058-5067.
8. (a) T. J. H. Vlugt, R. Krishna and B. Smit, *J. Phys. Chem. B*, 1999, **103**, 1102-1118; (b) S. Calero, D. Dubbeldam, R. Krishna, B. Smit, T. J. H. Vlugt, J. F. M. Denayer, J. A. Martens and T. L. M. Maesen, *J. Am. Chem. Soc.*, 2004, **126**, 11377-11386.
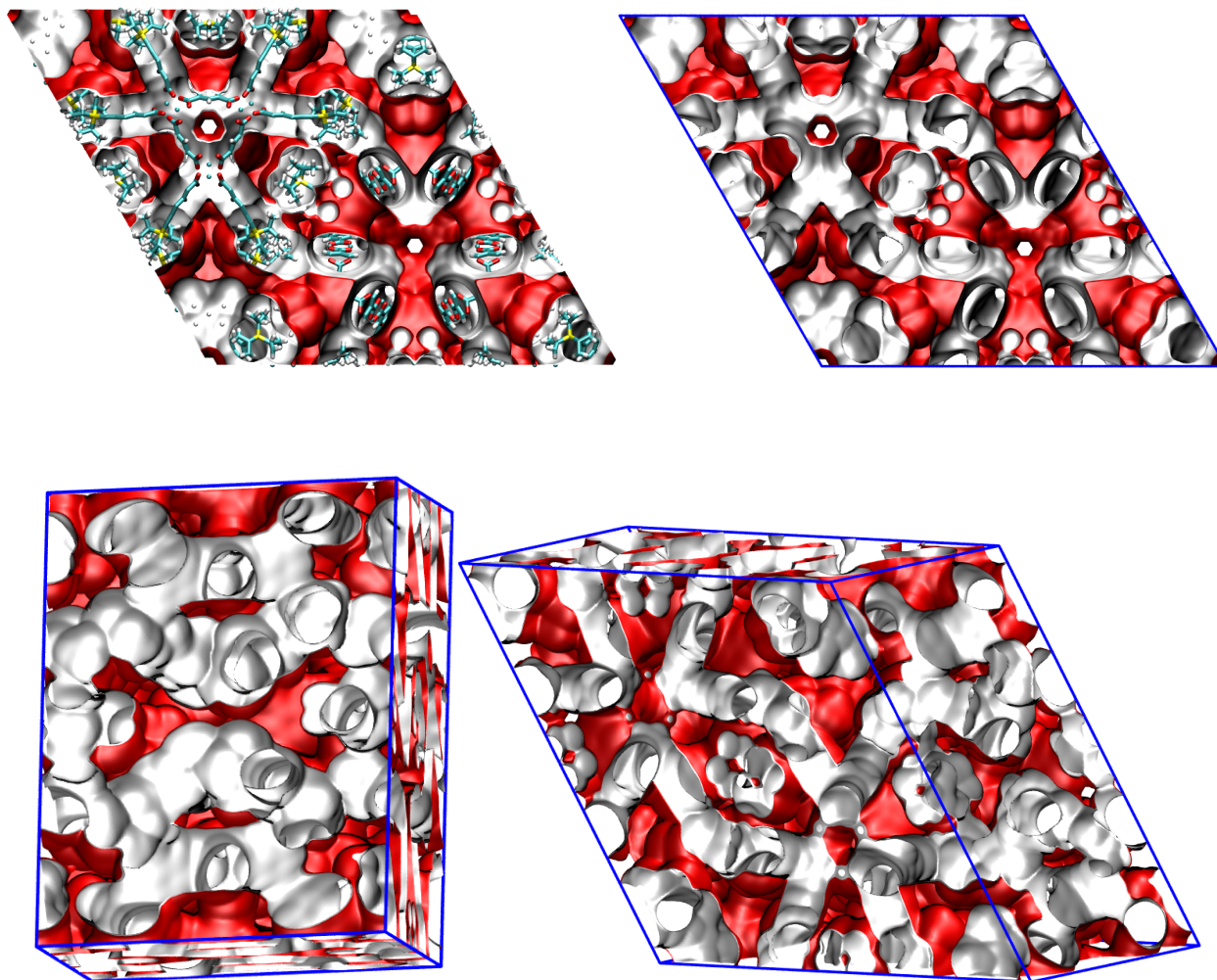9. A. L. Myers and J. M. Prausnitz, *AICHE J.*, 1965, **11**, 121-127.

Table S1. Lennard-Jones parameters for atoms in CuTEI.

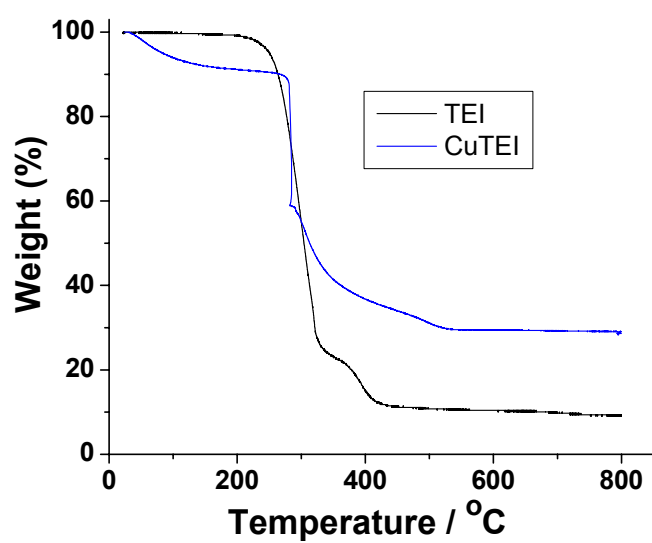| (pseudo-) atom	σ / Å	ε/k_B / K
Cu	3.11	2.52
O	3.03	48.16
C	3.47	47.86
Si	3.80	156.01
H	2.85	7.65

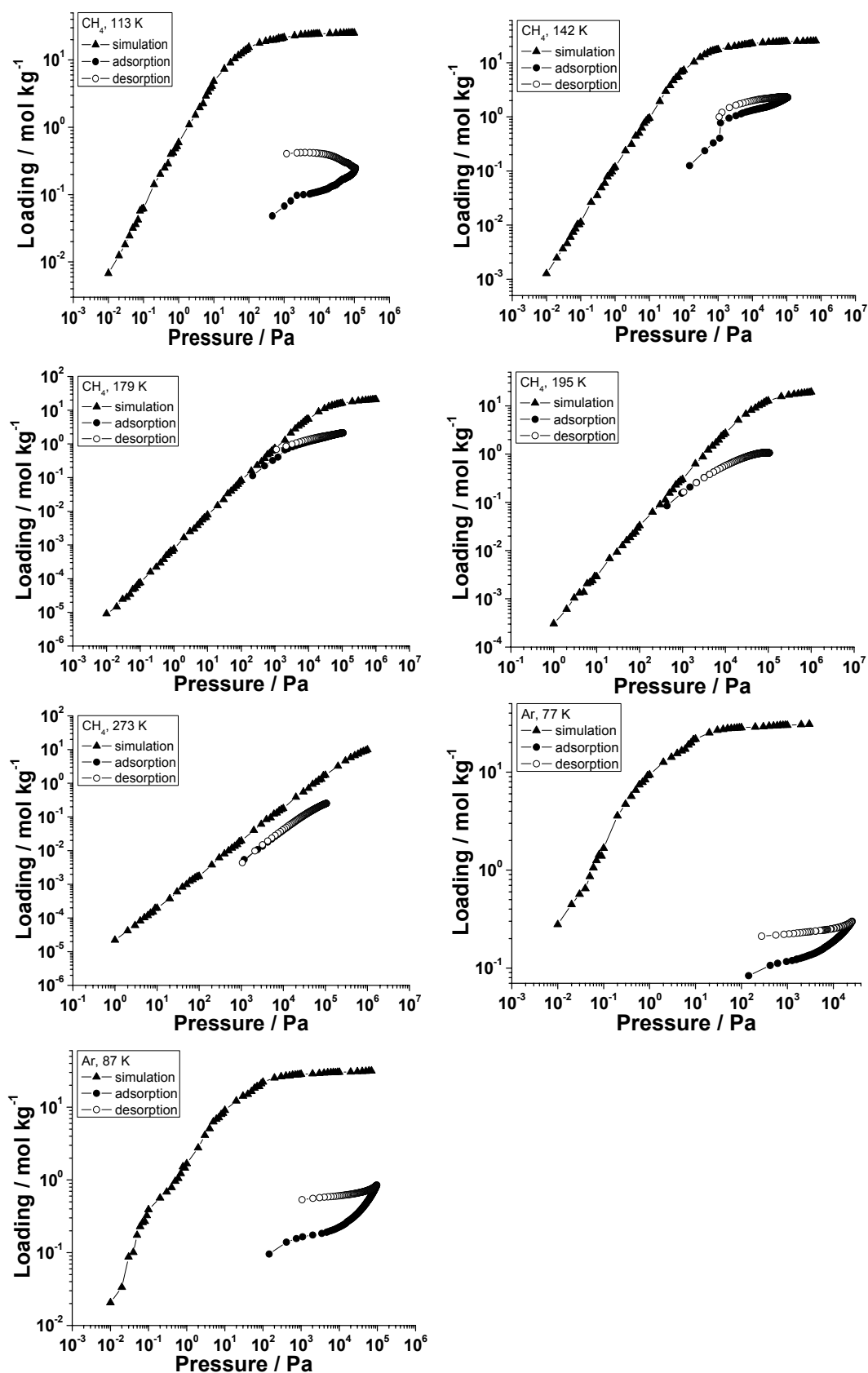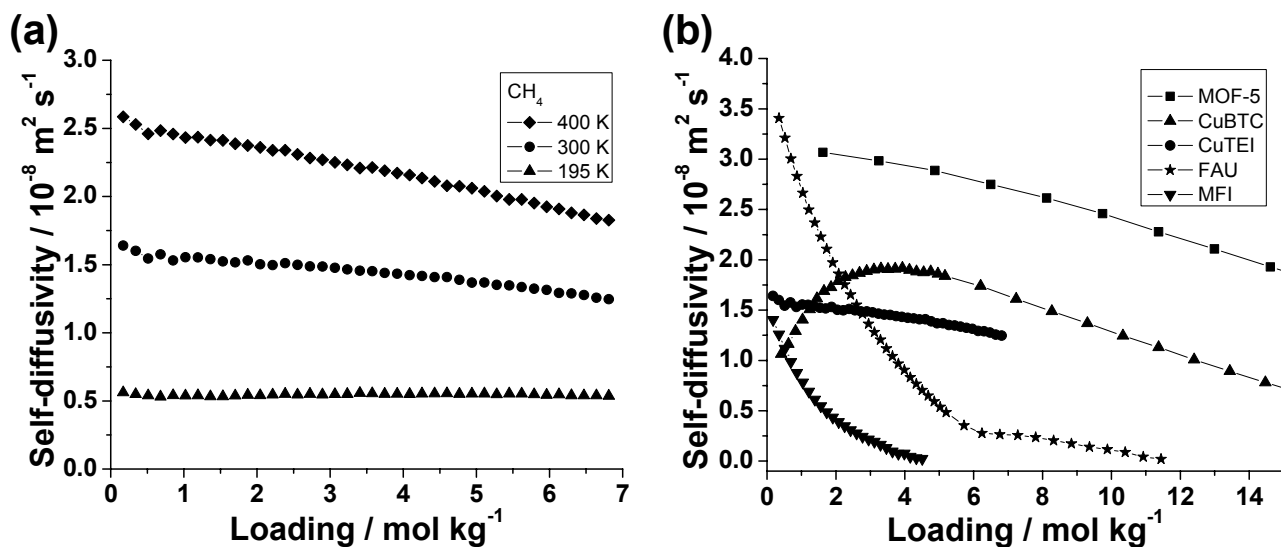See Cartoon below for further explanation:
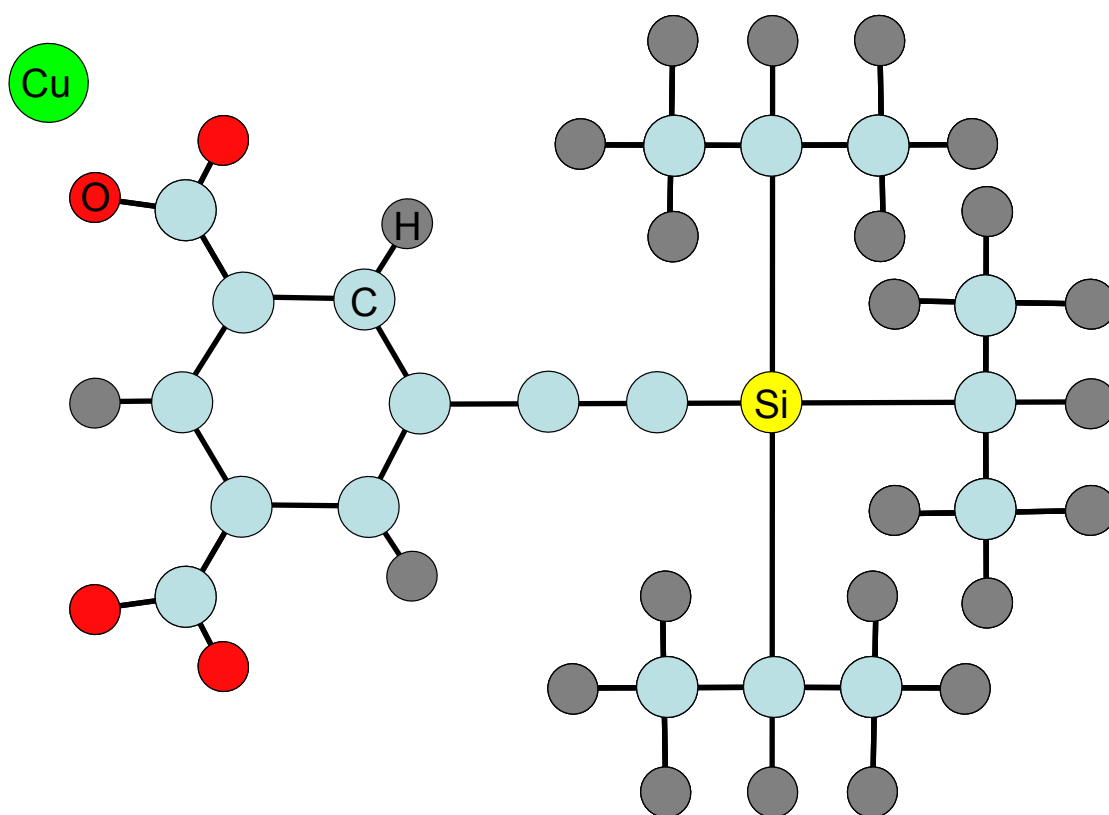
**Figure S1.** Pore landscapes of CuTEI (the red areas are accessible to guest molecules).

Figure S2. TGA curves of TEI and CuTEI.

Figure S3. Comparison of GCMC simulations of CH_4 and Ar isotherms for CuTEI with experimental

adsorption-desorption data.

Figure S4. (a) MD simulations for the self-diffusivity of CH_4 in CuTEI at 195 K, 300 K and 400 K. **(b)** Comparison of MD simulations for the self-diffusivity of CH_4 in CuTEI at 300 K with corresponding data for MOFs (MOF-5, CuBTC), and zeolites (FAU, MFI).
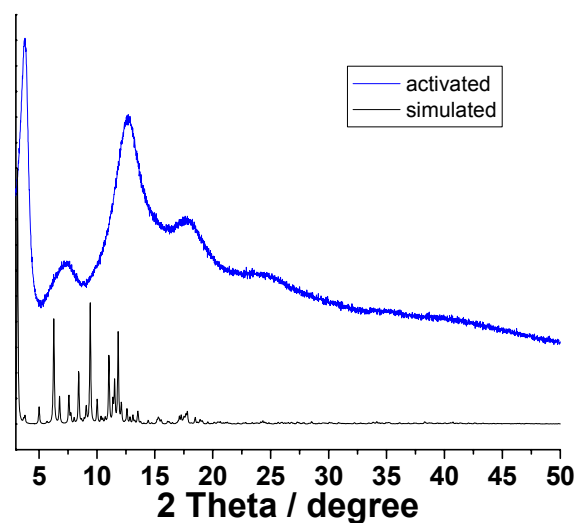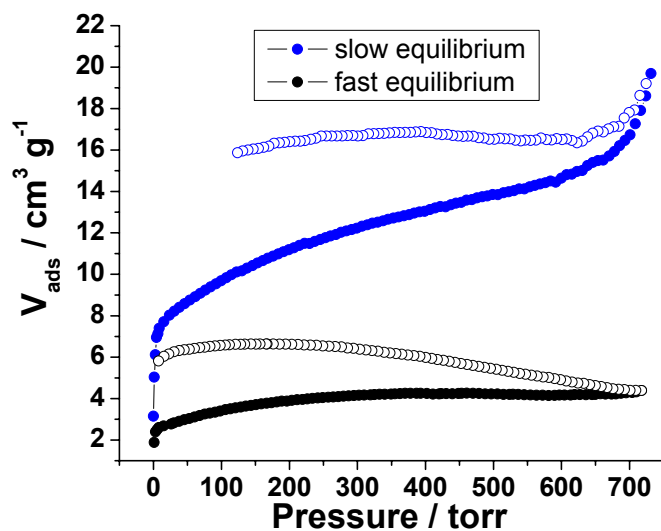

Figure S5. PXRD of CuTEI.

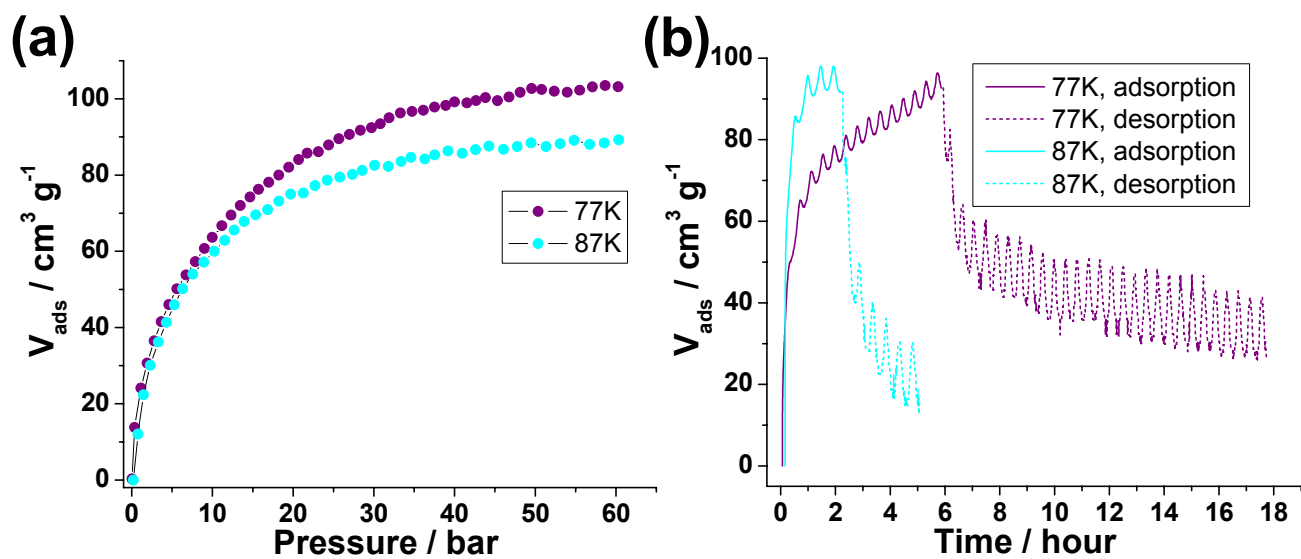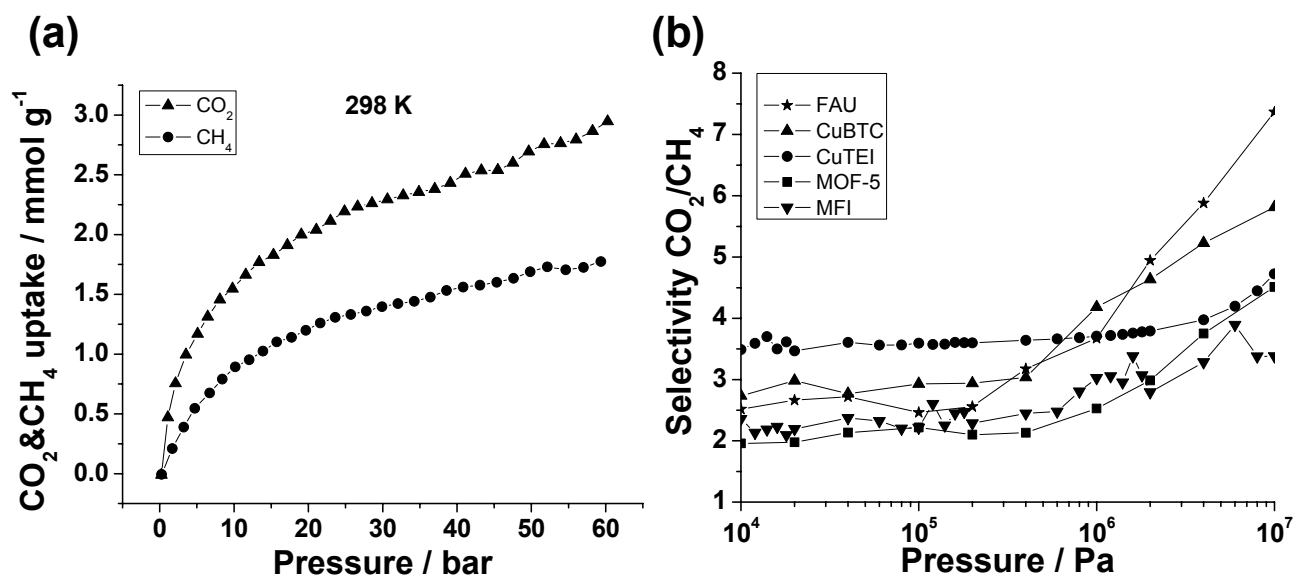**Figure S6.** N_2 sorption isotherms for CuTEI at 77 K under different equilibrium time (8 h *vs*. 65 h).

Figure S7. (a) High pressure H_2 adsorption isotherms for CuTEI. **(b)** H_2 sorption kinetics for CuTEI

(the zigzag noise comes from the temperature fluctuation of the gas reservoir).

Figure S8. (a) High pressure CO_2 and CH_4 adsorption isotherms for CuTEI at 298 K. **(b)** IAST

calculations of the adsorption selectivity for CO_2/CH_4 mixtures at 298 K in CuTEI as a function of the

total gas pressure for an equimolar mixture, $p_1=p_2$. Also shown are the adsorption selectivities for MOFs

(MOF-5, CuBTC) and zeolites (FAU, MFI) based on GCMC simulation results.